Delay effect on phase transitions in traffic dynamics

Takashi Nagatani and Ken Nakanishi
Division of Thermal Science, College of Engineering, Shizuoka University, Hamamatsu 432, Japan
(Received 24 November 1997)

A dynamical model of traffic is proposed to take into account the effect of acceleration delay. In the limit of no delay, the model reproduces the optimal velocity model of traffic. When the delay is small, it is shown that the phase transition among the freely moving phase, the coexisting phase, and the uniform congested phase occurs below the critical point. Above the critical point, no phase transition occurs. The value a_c of the critical point increases with increasing delay time $1/b$, where a is the friction coefficient (or sensitivity parameter). When the delay time is longer than $\frac{1}{2}$, the critical point disappears and the phase transition always occurs. The linear stability theory and nonlinear analysis are applied. The critical point predicted by the linear stability theory agrees with the simulation result. The modified Korteweg–de Vries (KdV) equation is obtained from the nonlinear analysis near the critical point. The phase separation line obtained from the modified KdV equation is consistent with the simulation result. [S1063-651X(98)03706-4]

PACS number(s): 05.70.Fh, 05.70.Jk, 89.40.+k

I. INTRODUCTION

Recently, traffic problems have attracted considerable attention [1]. Knowing the properties of a traffic jam is important in our life. Traffic jams are classified into two types: one is the spontaneous jam and the other is the causal jam. A causal jam is induced by such hindrances as car accidents, tunnels, and slopes. A spontaneous jam appears in congested traffic without the hindrances. Traffic jams have been studied by several traffic models: car following models [2–5], cellular automaton models [6–19], gas kinetic models [20–25], and hydrodynamic models [26,27].

The transition between the spontaneous jam and freely moving traffic has been investigated by several researchers. Nagel and Schreckenberg [6] have proposed the cellular automaton model for the transition to the spontaneous jam. Kerner and Konhauser [26] have presented the hydrodynamic model. Bando *et al.* [2] have proposed the optimal velocity model of traffic as an extended version of the car following models. In these models, jamming transitions between the freely moving phase and the jammed phase have been found. Furthermore, it has been shown that there exists a hysteresis near the transition point in the fundamental diagram. Recently, Krauss, Wagner, and Gawran [28] have found that there is a metastable region near the transition point in the Gipps model. It is known that the hysteresis phenomenon is due to the metastability. Barovic *et al.* [29] have showed that the metastability occurs in an extended version of the Nagel-Schreckenberg model. Kurtze and Hong [30] have derived the Korteweg–de Vries equation from the fluid dynamic traffic model to describe the traffic jam. Komatsu and Sasa [31] have derived the modified Korteweg–de Vries (MKdV) equation from the optimal velocity model to describe the kink-antikink density wave (traffic jam). It has been found that there is a critical point in the hydrodynamic and optimal velocity models. The phase transition occurs below the critical point. Near the critical point, the characteristic length and time scale as $(a_c-a)^{-1/2}$ and $(a_c-a)^{-3/2}$. The scaling exponents in the optimal velocity model are consistent with those in the fluid dynamic model.

Very recently, Nagatani presented the power-law model to describe the traffic jams [32]. The power-law model is an extended version of the optimal velocity model. It was shown that the phase transition and critical behaviors depend strongly on the power. The phase transition and critical behavior are definitely different from the other models. It was found that the scaling exponents are different from those of the optimal velocity model. The power-law model of traffic belongs to the different universality class from the optimal velocity and hydrodynamic models.

Generally, when a driver accelerates one's car, a delay occurs due to the car performance or driver's adjustment. The delay may have an important effect upon the property of traffic flow. In particular, we are interested in the effect of delay upon the jamming transition. There is an open question whether or not the delay affects effectively the traffic flow.

In this paper we present a dynamical traffic model to take into account the effect of acceleration delay. We investigate the effect of delay upon the phase transition and critical phenomenon by using computer simulation, the linear stability theory, and the nonlinear analysis. We show that the phase transition depends largely on the delay time of acceleration. We calculate the neutral stability line and the critical point from the linear stability theory. We derive the MKdV equation for describing the traffic jam. We compare the simulation result with the analytical result. We show the similarity between the jamming transition and the conventional liquid-gas phase transition. We discuss the similarity between the metastability and the spinodal decomposition.

The organization of the paper is as follows. In Sec. II we propose a dynamic traffic model taking into account the delay. In Sec. III we give the simulation result. The dependence of the critical point on the delay time is shown. The phase separation line is calculated and its dependence on the delay time is shown. In Sec. IV the stability of uniform traffic flow is analyzed by the linear stability theory. The neutral stability line and critical point are obtained. In Sec. V we apply the nonlinear analysis to the traffic flow near the critical point. We derive the MKdV equation for the traffic jam. The phase

separation line is calculated by the nonlinear wave equation. Section VI give a summary.

II. DYNAMIC MODEL

We propose a dynamical traffic flow model. The model is an extended version of the optimal velocity model proposed by Bando *et al.* [2]. A driving force acts on the car to accelerate it. Simultaneously, a friction force acts on the car. We assume that the driving force depends on the headway and time. The equation of motion of car j is

$$d^2x_j/dt^2 = A(\Delta x_j, t) - a\,dx_j/dt, \tag{1}$$

where x_j is the position of car j, Δx_j $(=x_{j-1}-x_j)$ is the headway, and a is the friction coefficient. $A(\Delta x_j, t)$ represents the driving force to accelerate car j. The second term on the right-hand side represents the friction force. We assume that the car velocity becomes the optimal velocity $V(\Delta x_j)$ in the steady state with no jam. The driving force approaches to $aV(\Delta x_j)$ after sufficiently large times. We call $aV(\Delta x_j)$ the *optimal driving force*. It is assumed that the driving force approaches $aV(\Delta x_j)$ with a first-order delay $1/b$. Then the equation of the driving force is

$$dA/dt = b\{aV(\Delta x_j) - A\}, \tag{2}$$

with

$$V(\Delta x_j) = \tanh(\Delta x_j - x_c) + \tanh x_c, \tag{3}$$

where x_c is the safety distance and $1/b$ represents the delay time. $V(\Delta x_j)$ represents the optimal velocity. The optimal velocity function (3) is consistent with that of Bando *et al.* [2]. If a jam does not occur, the car velocity becomes the optimal velocity $V(\Delta x_j)$ in the steady state. In the limit of $b \to \infty$, our model described by Eqs. (1)–(3) reproduces the original optimal velocity model proposed by Bando *et al.* [2]. This limit corresponds to the case of no delay when a driver accelerates one's car. In the optimal velocity model, the friction coefficient a is called the sensitivity. With decreasing b, the delay time $1/b$ increases. Then it takes more time for the driving force to approach the optimal driving force. In this model the maximal and minimal velocities are two and zero, respectively. The optimal velocity increases monotonically from the minimal velocity to the maximal velocity with increasing headway Δx_j. By introducing the delay, it is expected that the traffic flow changes effectively with the delay. In the following sections, we investigate the traffic properties of the model described by Eqs. (1)–(3).

III. SIMULATION AND RESULT

We study the phase transition in the model described by Eqs. (1)–(3). We perform a numerical simulation for the model. Initially, cars are randomly distributed on the one-dimensional space with car density ρ and initial velocity v_0. The boundary is periodic. In order to form a single jam, a hindrance is put at a point on the one-dimensional space. We assume that when a car reaches the hindrance it slows down instantly to low velocity v_h. In time, a single jam is formed just behind the hindrance. After the jam is formed, the hindrance is removed. The jam propagates backward with constant propagation velocity v_p. Once the single jam is formed for a special range of density, the jam is stable and does not break up. The jam has the symmetric form of the kink-antikink density wave. The stable jam occurs at an intermediate density. For low density, a jam disappears in time and all cars move freely with nearly maximal velocity. For high density, a jam also disappears in time and a congested uniform traffic flow occurs. Thus we can make a stable jam on the one-dimensional space for special values of density. We take the number of cars to be 100–400. The safety distance is set to $x_c = 5.0$.

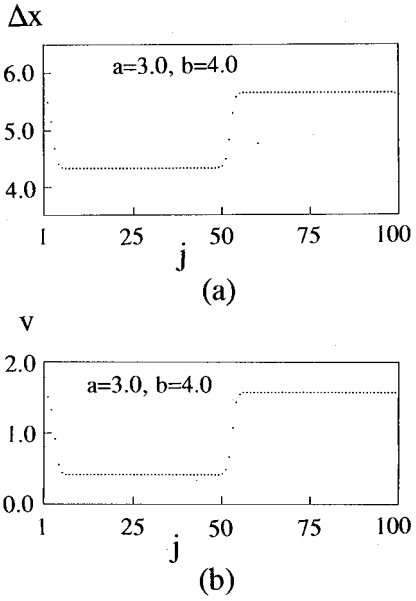

FIG. 1. Typical plots of the headway and velocity against numbered car j for total car number 100, car density $\rho = 0.2$, safety distance $x_c = 5.0$, $a = 3.0$, and $b = 4.0$. (a) and (b) indicate the profiles of headway and velocity, respectively, after sufficiently long times. A stable density wave is observed with the kink-antikink form. The density wave has a symmetric form. The density wave represents the traffic jam. The region with the short headway and low velocity indicates the traffic jam. The density wave propagates backward (from left to right) whereas cars move from right to left.

Figure 1 shows typical plots of the headway and velocity against numbered car j for total car number 100, car density $\rho = 0.2$, safety distance $x_c = 5.0$, $a = 3.0$, and $b = 4.0$. Figures 1(a) and 1(b) indicate the profiles of headway and velocity, respectively, after sufficiently long times. A stable density wave appears with the kink-antikink form. The density wave has a symmetric form. The region with the short headway and low velocity indicates the traffic jam. The region represents the density wave. The density wave propagates backward (from left to right) whereas cars move from right to left.

Figure 2 shows the plot of maximal headway $\Delta x_{\max}$ and minimal headway $\Delta x_{\min}$ against friction coefficient a for $b = 4.0$ where density $\rho = 0.2$, safety distance $x_c = 5.0$, and the total car number is 400. The headway out of the jam is nearly constant, but we choose the maximal value. Similarly, the headway within the jam is nearly constant, but we choose the minimal value. We calculate the maximal and minimal headways when a density wave (traffic jam) occurs. The circular points indicate the simulation results. For a special range of

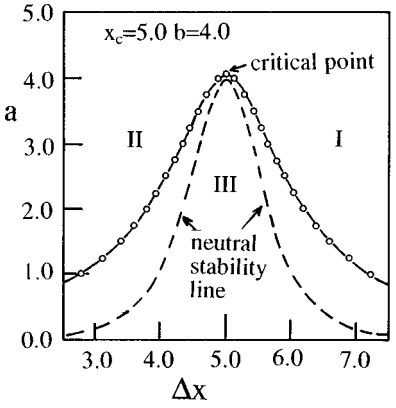

FIG. 2. Plot of maximal headway $\Delta x_{\max}$ and minimal headway $\Delta x_{\min}$ against friction coefficient a for $b=4.0$ where density $\rho=0.2$, safety distance $x_c=5.0$, and the total car number is 400. The circular points indicate the simulation result. Also represented is the phase diagram indicating the freely moving phase, the coexisting phase, and the uniform congested phase. Regions I, II, and III indicate, respectively, the freely moving phase, the uniform congested phase, and the coexisting phase in which the density wave appears. There is a critical point. It is given by $a_c=4.05\pm0.05$ for $b=4.0$. When the friction coefficient a is larger than $a_c=4.05$, the phase transition does not occur. The broken line indicates the neutral stability line obtained by the linear stability theory.

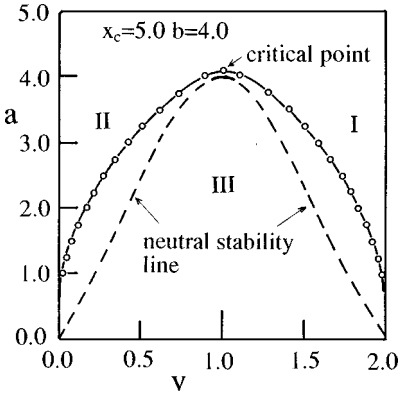

FIG. 3. Plot of maximal velocity $v_{\max}$ (out of the jam) and minimal velocity $v_{\min}$ (within the jam) against friction coefficient a for $b=4.0$ (for the same parameters as in Fig. 2). The circles indicate the simulation result. The data points are obtained by the same simulation result as in Fig. 2. The broken line indicates the neutral stability line. Regions I, II, and III indicate, respectively, the freely moving phase, the uniform congested phase, and the coexisting phase.

density, a jam appears. When a stable jam occurs, the maximal and minimal headways give the same values for a constant value of a. The maximal and minimal headways do not depend on the density. However, for low density, a jam does not occur. The limit of density in which no jam occurs is given by the inverse of the headway when no density wave appears. The boundary between the jam and no jam is consistent with the solid curve on the right-hand side in Fig. 2. Also, the boundary between the jam phase and the uniform congested phase is given by the solid curve on the left-hand side in Fig. 2. In Fig. 2, region I above the phase boundary on the right-hand side indicates the freely moving phase. Region II above the phase boundary on the left-hand side indicates the uniform congested traffic flow without a density wave. In region III inside both phase boundaries, the coexisting phase with a density wave appears. In the coexisting phase, the freely moving phase coexists with the congested phase. In the coexisting phase, the typical profiles of headway and velocity are shown in Fig. 1. Thus Fig. 2 shows the phase diagram representing the freely moving phase, the coexisting phase, and the uniform congested phase. There is a critical point, which is given by $a_c=4.05\pm0.05$ for $b=4.0$. When the friction coefficient a is larger than $a_c=4.05$, no density wave appears. For $a>a_c$, the phase transition does not occur. The broken line indicates the neutral stability line obtained by the linear stability theory. The linear stability analysis is given in Sec. IV. The critical point predicted by the linear stability theory is given by $a_c=4.0$ for $b=4.0$. The value a_c of the critical point obtained from simulation is consistent with that predicted by the linear stability theory within numerical accuracy.

Similarly, Fig. 3 shows the plot of maximal velocity $v_{\max}$ (out of the jam) and minimal velocity $v_{\min}$ (within the jam) against the friction coefficient a for $b=4.0$ (for the same parameters as in Fig. 2). The circles indicate the simulation result. The data points are obtained by the same simulation as in Fig. 2. Figure 3 also represents the phase diagram indicating the freely moving phase, the coexisting phase, and the uniform congested phase. Above the critical point $a_c=4.05$, the phase transition does not occur. The broken line indicates the neutral stability line obtained by the linear stability theory. Regions I, II, and III indicate, respectively, the freely moving phase, the uniform congested phase, and the coexisting phase.

The following quantities define the order parameter S:

$$S=\Delta x_f-\Delta x_j \quad \text{or} \quad v_f-v_j, \tag{4}$$

where Δx_f is the headway out of the jam, Δx_j is the headway within the jam, v_f is the car velocity out of the jam, and v_j is the car velocity within the jam. The order parameter S is different from zero below the critical point a_c.

We discuss the similarity of the jamming transition to the conventional liquid-gas phase transition. We can interpret the sensitivity parameter a and headway Δx as temperature and volume, respectively. Our order parameter is similar to that in the conventional liquid-gas phase transition. The jammed phase and the freely moving phase correspond to the liquid phase and the gas phase, respectively. Figures 2 and 3 exhibit a phase diagram similar to the phase transition and critical phenomenon. The jamming transition has the properties common to the liquid-gas phase transition.

Figure 4 shows plots of the maximal headway and the minimal headway for $b=2$, 3, 4, 6, 8, and 100 where density $\rho=0.2$, safety distance $x_c=5.0$, and the total car number is 400. Figure 5 shows plots of the maximal velocity and the minimal velocity for $b=2$, 3, 4, 6, 8, and 100 (for the same values as in Fig. 4). With increasing delay time $1/b$ (decreasing b), the critical point increases. When $b\leqslant2.0$, there is no critical point. When delay time $1/b$ of the driving force is larger than 0.5, the critical point disappears. In the case of $b<2.0$, the phase transition always occurs even if a is sufficiently large. It is interesting that the critical point disappears for $b<2.0$. In the limit $b\to\infty$ (when the delay time

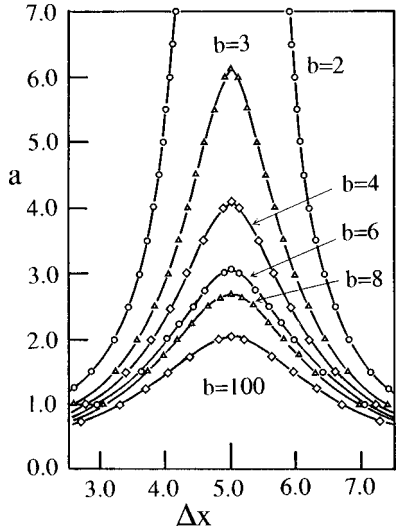

FIG. 4. Plots of the maximal headway and the minimal headway for $b=2$, 3, 4, 6, 8, and 100 where density $\rho=0.2$, safety distance $x_c=5.0$, and the total car number is 400.

approaches zero), the phase boundary agrees with that obtained by the original optimal velocity model.

Figure 6 shows a plot of the critical point a_c against b. The circles indicate the simulation result. The solid curve represents the critical points predicted by the linear stability theory. Its curve is given by $a_c=2b/(b-2)$. The simulation result is consistent with the linear stability result. The critical point diverges at $b=2.0$.

We discuss the metastability of the jamming transition in our model. We made the density wave start from a causal jam induced by the slowing down. The phase diagram between the sensitivity parameter a and headway Δx was obtained from the density wave. If we start from a uniform state and add a disturbance at a point to the uniform state, the density wave does not always appear even when the density is between the phase separation line and the neutral stability line. In the region between the phase separation line and the neutral stability line, the appearance of density waves (traffic jams) depends strongly on the strength of the distrurbance.

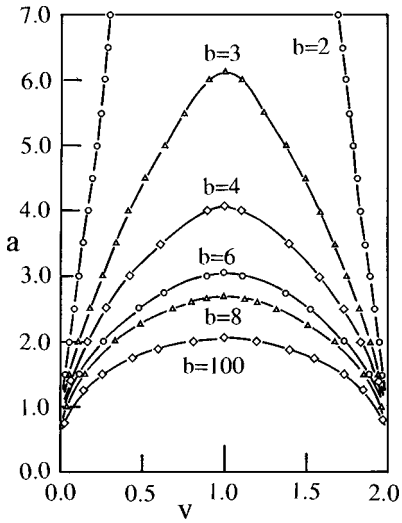

FIG. 5. Plots of the maximal velocity and the minimal velocity for $b=2$, 3, 4, 6, 8, and 100 (for the same parameters as in Fig. 4).

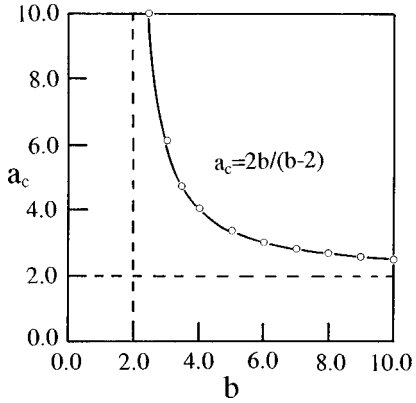

FIG. 6. Plot of critical point a_c against b. The circles indicate the simulation result. The solid curve represents the critical points predicted by the linear stability theory. Its curve is given by $a_c=2b/(b-2)$. The simulation result is consistent with the linear stability result. The critical point diverges at $b=2.0$.

Its region corresponds to the region of the metastable states II. The neutral stability line corresponds to the spinodal line in the conventional phase transition. In the region of unstable states between the neutral lines (broken lines) within the coexisting phase, the density wave always appears when the same distrurbance is added to the uniform state (see Fig. 2). Indroducing the delay into the original optimal velocity model, the region of the metastable states changes significantly (see Figs. 4 and 10).

IV. LINEAR STABILITY THEORY

We apply the linear stability theory to our model. We consider the stability of a uniform traffic flow. The uniform traffic flow is defined by such a state that all cars move with constant headway h and optimal velocity $V(h)$. The solution $x_{j,0}$ of the uniform steady state is obtained by taking $d^2x_j/dt^2=0$ and $dA_j/dt=0$:

$$x_{j,0}=hj+V(h)t \quad \text{with} \quad h=L/N, \tag{5}$$

where $A_{j,0}=aV(h)$, N is the number of cars, L is the system size, and h is the car spacing (identical headway). Let y_j and w_j be small deviations from the steady-state solutions $x_{j,0}$ and $A_{j,0}$: $x_j=x_{j,0}+y_j$ and $A_j=A_{j,0}+w_j$. Then the linear equations are obtained

$$d^2y_j/dt^2=w_j-ady_j/dt,$$

$$dw_j/dt=b[aV'(h)\Delta y_j-w_j], \tag{6}$$

where $V'(h)$ is the derivative of optimal velocity $V(\Delta x)$ at $\Delta x=h$. By expanding $y_j=Y\exp(ikj+zt)$ and $w_j=W\exp(ikj+zt)$, one obtains

$$\begin{pmatrix} z^2+az & -1 \\ -abV'(h)(e^{ik}-1) & z+b \end{pmatrix}\begin{pmatrix} Y \\ W \end{pmatrix}=0. \tag{7}$$

By the condition of nontrivial solutions, one obtains

$$z^3+(a+b)z^2+abz-abV'(h)(e^{ik}-1)=0. \tag{8}$$

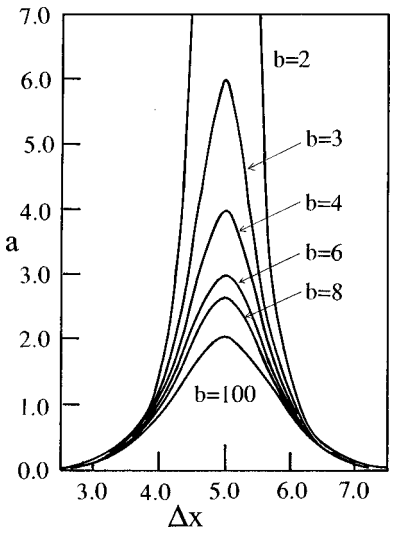

FIG. 7. Neutral stability curves in the $(\Delta x,a)$ plane for $b=2.0$, 3.0, 4.0, 6.0, 8.0, and 100.

By setting $z_1=0$ (z_1 is the real part of z), the neutral stability condition is obtained. At the $k\approx 0$ mode, the uniform traffic flow is unstable for

$$V'(h)>\alpha/2, \tag{9}$$

where $1/\alpha=1/a+1/b$.

Hereafter, we call α the effective sensitivity. Equation (9) tells us that the stability condition for effective sensitivity α is given by $2V'(h)$, as in the original optimal velocity model. In the limit $b\to\infty$, Eq. (9) reduces to that obtained by the optimal velocity model. Since $V'(h)$ has a maximal value 1 at $h=x_c$, a uniform traffic flow is always stable if the following condition is satisfied:

$$a>2b/(b-2) \quad \text{for} \quad b>2.0. \tag{10}$$

When a small disturbance is added to the uniform flow (with a constant headway and the optimal velocity) satisfying the above condition, its uniform flow is always stable. We find that there is a critical point a_c for $b>2.0$. The critical point is given by

$$a_c=2b/(b-2) \quad \text{for} \quad b>2.0. \tag{11}$$

If $b\leqslant 2.0$, there is no critical point and the uniform traffic flow is always unstable. The neutral stability condition is given by $V'(h)=ab/[2(a+b)]$. Figure 7 shows the neutral stability lines in the $(\Delta x,a)$ plane for $b=2.0$, 3.0, 4.0, 6.0, 8.0, and 100. With increasing delay time $1/b$, the critical point increases. When $b\leqslant 2.0$, there is no critical point. For comparison with the simulation result, the neutral stability lines are shown by the broken lines in Figs. 2 and 3. The dependence of critical point upon b is shown by the solid line in Fig. 6. The critical point predicted by Eq. (11) agrees with the simulation result. For later convenience, let us derive the long-wavelength expansion of z in the vicinity of the neutral stability curve, which is determined order by order around $ik\sim 0$:

$$z(ik)=iV'k+\frac{\alpha_c-\alpha}{4}k^2-i\frac{V'}{6}\left(1-\frac{6V'^2}{ab}\right)k^3 - \frac{V'}{8}\left(1-\frac{8V'^2}{ab}\right)k^4, \tag{12}$$

where $\alpha_c=2$.

V. NONLINEAR ANALYSIS

We derive the weakly nonlinear wave equation of the jam formation, using the reductive perturbation method. We eliminate the driving force A from Eqs. (1) and (2) and obtain the third-order differential equation for x_j,

$$\partial_t^3 x_j+(a+b)\partial_t^2 x_j+ab\partial_t x_j=abV(\Delta x_j). \tag{13}$$

To consider the deviation from the uniform flow with headway h, we define $r(x,t)=\Delta x_j(t)-h$, where $x=jh$:

$$\begin{aligned}[\partial_t^3+(a+b)\partial_t^2+ab\partial_t]r(x,t)&=ab[V(h+r(x+h,t)) \\ &\quad -V(h+r(x,t))] \\ &=ab(e^{h\partial_x}-1) \\ &\quad \times V(h+r(x,t)).\end{aligned} \tag{14}$$

We collect the linear terms for r on the left-hand side as

$$\begin{aligned}[\partial_t^3+(a+b)\partial_t^2+ab\partial_t-abV'(h)(e^{h\partial_x}-1)]r \\ =ab(e^{h\partial_x}-1)N[r],\end{aligned} \tag{15}$$

where

$$N[r]=\sum_{n=2}^{\infty}\frac{V^{(n)}(h)}{n!}r^n. \tag{16}$$

Here $V^{(n)}(h)$ denotes the nth derivative of the optimal velocity at headway h.

The differential operator on the left-hand side of Eq. (15) can be factorized as $(\partial_t-z)(\partial_t-z_1)(\partial_t-z_2)$, where z's satisfy

$$z+z_1+z_2=-(a+b), \quad (z_1+z_2)z+z_1z_2=ab. \tag{17}$$

$z(\partial_x)$ is given by Eq. (12), where ik is substituted by $h\partial_x$ and z_1,z_2 correspond to irrelevant decaying modes, whose real parts are negative. Then we can replace the differential operator with $(\partial_t-z)(\partial_t-z_1)(\partial_t-z_2)$ and rewrite the last two factors of it by using Eq. (17) as

$$\begin{aligned}(z-z_1)(z-z_2)&=3z^2+2(a+b)z+ab \\ &=ab(1+2z/\alpha+3z^2/ab).\end{aligned} \tag{18}$$

Thus we obtain the weakly nonlinear long-wavelength equation

$$(\partial_t-z)r=(1+2z/\alpha+3z^2/ab)^{-1}N[r]. \tag{19}$$

By numerical analysis, we already know that the critical point for the jam formation is at $\alpha=\alpha_c=2$ and $h=x_c$, where x_c is determined by the turning point $V''(x_c)=0$ of the

optimal velocity function, which corresponds to the top of the neutral stability curve. Then we will investigate Eq. (19) around the critical point by taking $\varepsilon^2=(\alpha_c-\alpha)/\alpha_c$. When we make the scaling ansatz

$$r(x,t)=2\varepsilon\sqrt{\frac{V'}{|V'''|}}\,R(y,\tau),$$

$$y=2\varepsilon\left(\frac{x}{h}+V't\right),$$

$$\tau=\tfrac{4}{3}\varepsilon^3V't, \tag{20}$$

we obtain the regularized equation

$$\partial_\tau R-f\partial_y^3R+\partial_yR^3=-\varepsilon M[R], \tag{21}$$

where

$$M[R]=\tfrac{3}{2}[\partial_y^2R+g\partial_y^4R-\tfrac{2}{3}\partial_y^2R^3], \tag{22}$$

$f=1-6V'^2/ab$, and $g=1-8V'^2/ab$. Note that hereinafter all derivatives of the optimal velocity are evaluated at $h=x_c$. It also should be noted that f and g are always positive for any a and b.

Let us find the propagating solution of Eq. (21) with constant velocity c by setting $R=R(y-c\tau)$. First, we ignore the $O(\varepsilon)$ terms in Eq. (21) and get the MKdV equation, which has the kink solution

$$R_0(y)=\sqrt{c}\,\tanh\sqrt{\frac{c}{2f}}\,y. \tag{23}$$

Next, assuming $R=R_0+\varepsilon R_1$, we take into account the $O(\varepsilon)$ correction and get for R_1

$$LR_1=M[R_0], \tag{24}$$

where

$$L=c\partial_y+f\partial_y^3-3R_0^2\partial_y-3\partial_yR_0^2. \tag{25}$$

To determine the selected value of the propagation velocity c for the kink solution (23), we consider the solvability condition for Eq. (24),

$$(\Phi_0,M[R_0])\equiv\int_{-\infty}^{+\infty}dy\;\Phi_0M[R_0]=0, \tag{26}$$

where Φ_0 is the zeroth eigenfunction of the adjoint operator $L^\dagger$,

$$L^\dagger\Phi_0=0,\quad L^\dagger=-c\partial_y-f\partial_y^3+3R_0^2\partial_y. \tag{27}$$

Fortunately, we find that the zeroth-order solution R_0 itself satisfies Eq. (27) and we can choose $\Phi_0=R_0$. Performing the integration, we obtain the selected velocity

$$c=5f/2(f+g). \tag{28}$$

When $b\to\infty$, f and g go to unity and we get $c=\frac{5}{4}$, which agrees with the result obtained by Komatsu and Sasa [31].

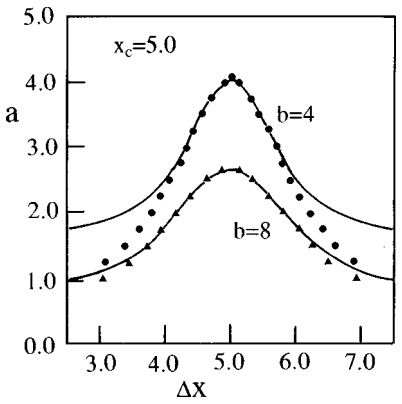

FIG. 8. Phase separation curves obtained by the nonlinear analysis for $b=4$ and 8. The curves obtained from Eq. (29) are indicated by solid lines. The simulation data for $b=4$ and 8 are plotted by full circles and triangles.

If we adopt the explicit form (3) of the optimal velocity, the amplitude ($\mathcal{A}$) of the kink solution is given by

$$\mathcal{A}=\varepsilon\sqrt{\frac{5f}{2(f+g)}}=\sqrt{5\left(\frac{a+b}{ab}-\frac{1}{2}\right)\frac{ab-6}{ab-7}}. \tag{29}$$

We show the result for $b=4$ and 8 in Fig. 8. The full circles and triangles indicate data points of simulation for $b=4$ and 8, respectively. The phase separation curves obtained analytically are indicated by the solid curves. The analytical result is in good agreement with the numerical simulation near the critical point.

VI. SUMMARY

We proposed the traffic flow model to describe the spontaneous traffic jam occurring on a highway. We extended the optimal velocity model to take into account the delay effect of the driving force. We investigated the jamming transition among the freely moving phase, the coexisting phase, and the uniform congested phase. We obtained the phase diagram for the phase transition and critical phenomenon. We showed that the delay of the driving force has an important effect upon the jamming transition. We found that there is no critical point when the delay time $1/b$ is longer than $\frac{1}{2}$.

We applied the linear stability theory to our model. We showed that the critical point can be predicted by the linear stability theory. We derived the MKdV equation to describe the traffic jam near the critical point, using the nonlinear analysis. It was shown that the phase separation curve predicted by the nonlinear wave equation is consistent with that obtained by the simulation.

We showed that there is a similarity between our jamming transition and the liquid-gas phase transition when sensitivity a and headway Δx correspond to the temperature and volume, respectively. Also, we discussed the similarity of the metastability to the spinodal decomposition. In order to describe more accurately the jamming transition in terms of the phase transition and critical phenomenon, it will be necessary to derive the time-dependent Ginzburg-Landau equation from the optimal velocity model.

[1] *Traffic and Granular Flow*, edited by D. E. Wolf, M. Schreckenberg, and A. Bachem (World Scientific, Singapore, 1996).
[2] M. Bando, K. Hasebe, A. Nakayama, A. Shibata, and Y. Sugiyama, Phys. Rev. E **51**, 1035 (1995).
[3] M. Bando, K. Hasebe, K. Nakanishi, A. Nakayama, A. Shibata, and Y. Sugiyama, J. Phys. I **5**, 1389 (1995).
[4] K. Nakanishi, K. Itoh, Y. Igarashi, and M. Bando, Phys. Rev. E **55**, 6519 (1997).
[5] Y. Sugiyama and H. Yamada, Phys. Rev. E **55**, 7749 (1997).
[6] K. Nagel and M. Schreckenberg, J. Phys. I **2**, 2221 (1992).
[7] M. Schreckenberg, A. Schadschneider, K. Nagel, and N. Ito, Phys. Rev. E **51**, 2329 (1995).
[8] K. Nagel and H. J. Herrmann, Physica A **199**, 254 (1993).
[9] G. Csanyi and J. Kertestz, J. Phys. A **28**, 427 (1995).
[10] S. C. Benjamin, N. F. Johnson, and P. M. Hui, J. Phys. A **29**, 3119 (1996).
[11] M. Takayasu and H. Takayasu, Fractals **1**, 860 (1993).
[12] M. Fukui and Y. Ishibashi, J. Phys. Soc. Jpn. **66**, 385 (1997).
[13] A. Schadschneider and M. Schreckenberg, Ann. Phys. (Leipzig) **6**, 541 (1997).
[14] H. Emmerich and E. Rank, Physica A **216**, 435 (1995); **234**, 676 (1997).
[15] O. Biham, A. A. Middleton, and D. A. Levine, Phys. Rev. A **46**, R6124 (1992).
[16] T. Nagatani, Phys. Rev. E **48**, 3290 (1993).
[17] J. A. Cuesta, F. C. Matinez, J. M. Molera, and A. Sanchez, Phys. Rev. E **48**, 4175 (1993).
[18] K. H. Chung, P. M. Hui, and G. Q. Gu, Phys. Rev. E **51**, 772 (1995).
[19] T. Nagatani, Phys. Rev. E **51**, 922 (1995).
[20] I. Prigogine and R. Herman, *Kinetic Theory of Vehicular Traffic* (Elsevier, New York, 1971).
[21] S. L. Paveri-Fontana, Transp. Res. **9**, 225 (1975).
[22] E. Ben-Naim, P. L. Krapivsky, and S. Redner, Phys. Rev. E **50**, 822 (1994).
[23] D. Helbing, Phys. Rev. E **53**, 2366 (1996).
[24] D. Helbing, Physica A **233**, 253 (1996).
[25] T. Nagatani, Physica A **237**, 67 (1997).
[26] B. S. Kerner and P. Konhauser, Phys. Rev. E **48**, 2335 (1993).
[27] B. S. Kerner, P. Konhauser, and M. Schilke, Phys. Rev. E **51**, 6243 (1995).
[28] S. Krauss, P. Wagner, and C. Gawron, Phys. Rev. E **55**, 5597 (1997).
[29] R. Barovic, L. Santen, A. Schadschneider, and M. Schreckenberg (unpublished).
[30] D. A. Kurtze and D. C. Hong, Phys. Rev. E **52**, 218 (1995).
[31] T. Komatsu and S. Sasa, Phys. Rev. E **52**, 5574 (1995).
[32] T. Nagatani, Physica A **246**, 460 (1997).